Hard-mode Raman spectroscopy and structural phase transition in the relaxor ferroelectric

lead scandium tantalate, $Pb(Sc_{0.5}Ta_{0.5})O_3$

Hard-mode Raman spectroscopy and structural phase transition in the relaxor ferroelectric lead scandium tantalate, Pb(Sc$_{0.5}$Ta$_{0.5}$)O$_3$

U Bismayer†, V Devarajan‡ and P Groves§

† Institut für Mineralogie und Sonderforschungsbereich 173 der Universität Hannover, Welfengarten 1, D-3000 Hannover 1, Federal Republic of Germany
‡ Department of Physics, Pondicherry University, JIPMER Campus, Pondicherry-605006, India
§ Alcan International Ltd, Banbury Laboratories, Banbury, Oxon OX16 7SP, UK

Abstract. The phase transition in the relaxor ferroelectric lead scandium tantalate, Pb(Sc$_{0.5}$Ta$_{0.5}$)O$_3$, is investigated in both ordered and partly disordered (Sc, Ta disorder) modifications through the technique of hard-mode Raman spectroscopy. The vibrational modes for ordered para phase, ordered ferroelectric phase, disordered para phase and disordered ferroelectric phase are assigned to different representations of the respective groups (Fm$\bar{3}$m ($Z = 2$), R3m ($Z = 2$), Pm$\bar{3}$m ($Z = 1$) and R3m ($Z = 1$)) using the usual group-theoretical methods. The temperature evolution of the strong Raman band at 61 cm^{-1} (hard mode) is investigated from 102 K to 873 K, for both phase transitions, namely ordered para to ordered ferro and disordered para to disordered ferro phases. The temperature variations of integrated intensity, full width at half maximum and square of the frequency of the 61 cm^{-1} band are discussed in the light of phase transition mechanisms involved in relaxor ferroelectrics for both cases.

1. Introduction

Pb(Sc$_{0.5}$Ta$_{0.5}$)O$_3$ (PST) shows a critical behaviour characteristic for diffuse ferroelectrics of the perovskite-type ABO$_3$. The distribution of two inequivalent B cations Sc^{3+} and Ta^{5+} can be varied by isothermal annealing (Setter and Cross 1980, Stenger and Burgraff 1980). The so-controlled degree of order affects the physical properties of the compound considerably. The dielectric behaviour of disordered crystals shows a broad relaxor character over the Curie range whereas the dielectric constant of ordered PST shows a discontinuous behaviour as a function of temperature (Setter and Cross 1981). Annealing (i.e. ordering) of lead scandium tantalate crystals with ideal cubic high-temperature symmetry produces a doubling of the lattice constant $a_0 \rightarrow 2a_0$ ($a_0 = 4.0760$ Å at $T = 295$ K) (Groves 1985, Randall *et al* 1986). This results in alternating Sc and Ta cations occupying B sites and consequently a face centring of the lattice is achieved. TEM studies on PST by Randall *et al* (1986) and x-ray measurements on lead indium niobate by Groves (1986) revealed the existence of micro-domains in the heat-treated crystals. By varying the annealing time these ferroelectric domains associated with the structural order in the material could be increased up to an average size of 200 nm. Generally in this

compound the degree of order determines the symmetry of the stable phase, i.e. the ferroelectric low-temperature phase and the paraelectric high-temperature phase. Recently Salje and Bismayer (1989) investigated the group–subgroup relations involving the transition of ordered and disordered PST to their respective low-temperature phases using Landau theory. To describe non-equilibrium states in a non-homogeneous matrix the authors considered the corresponding ferroelectric and the ferroelastic ordering schemes separately, including their mutual coupling. Hence, they interpreted the ferro-electric and ferroelastic phase transformations as two steps of a cascade of phase transitions involving symmetry reductions to the respective maximal subgroups. They show the following symmetry reductions:

(i) Pm$\bar{3}$m–R$\bar{3}$m–R3m for the disordered paraelectric (Pm$\bar{3}$m, $Z = 1$) to disordered ferroelectric (R3m, $Z = 1$) transition. R$\bar{3}$m represents a ferroelastic modification that appears in the sequence of phase transitions.

(ii) Fm$\bar{3}$m–R$\bar{3}$m–R3m for the ordered paraelectric (Fm$\bar{3}$m, $Z = 2$) to ordered ferro-electric (R3m, $Z = 2$) transition. R$\bar{3}$m ($Z = 2$) again represents a ferroelastic phase which appears during the symmetry reduction.

Disordered PST undergoes a paraelectric–ferroelectric transition near 270 K (Groves 1985). The transition temperature increases with increasing degree of order (Stenger and Burggraaf 1980). In both the transitions mentioned above the structure of the low-temperature unit cell is based upon a pseudo-cubic $2a_0 \times 2a_0 \times 2a_0$ superlattice cell where ferroelectricity is introduced by static displacements of lead atoms along the [111] direction giving rise to a total number of eight ferroelectric domains in the rhombohedral phase. Several theoretical attempts have been made to describe the physical mechanism involved in this phase transformation. Originally, different models were proposed to explain the relaxor-type of the phase transformation in this material:

(i) the compositional fluctuation model (Smolensky 1970) which is based on the assumption of spatial compositional changes, and

(ii) the localised deviations from long-range order model (Burns 1976, Reinecke and Ngai 1976) which involves localised structural perturbations in a stoichiometric homogeneous compound.

More recently Burns and Dacol (1983, 1986) carried out Raman and infrared studies on Pb(Mg$_{1/3}$Nb$_{2/3}$)O$_3$ and Pb(Ti$_{0.85}$Sn$_{0.15}$)O$_3$ crystals and concluded that in these crystals compositional fluctuations over larger crystal regions do not play a major role in the phase transition. The authors investigated the refractive index behaviour in these systems as a function of temperature ($n(T)$) and suggested that there may be glassy polarisation behaviour far above the observed transformation point in these compounds. Their data support the assumption that above T_c the translational symmetry is broken which stabilises regions of local polarisation of static or dynamic character.

Early Raman spectroscopic investigations on relaxor ferroelectrics (e.g. Pb(Mg$_{0.5}$W$_{0.5}$)O$_3$ and Pb$_3$(MgTa$_2$)O$_9$) have been made by Smolensky *et al* (1976). However, so far no such studies have been carried out on lead scandium tantalate.

A technique which was shown to be particularly sensitive to detect changes in the structural short-range order, e.g. sublattice polarisation and ordering processes, is hard-mode Raman spectroscopy as previously described by Bruce *et al* (1980), Salje *et al* (1983), Devarajan and Salje (1986) and Bismayer (1988). The influence of the density of states fluctuations on the scattering of hard modes was demonstrated by Salje (1986) and Bismayer *et al* (1986). The experimental procedure described by Bismayer (1988)

was adopted here to study the paraelectric–ferroelectric phase transformation of PST (both ordered and disordered crystals).

2. Experimental

For Raman spectroscopic measurements samples of Pb(Sc$_{0.5}$Ta$_{0.5}$)O$_3$ with a size of about $2 \times 2 \times 2$ mm^3 were used. The multi-domain crystals were grown from flux as described by Setter and Cross (1980). To order the samples they were annealed at 975 K in gas-tight platinum crucibles. To keep PbO loss to a minimum the annealing time was limited to 15 h. X-ray microanalysis by TEM/EDS revealed no measurable change in lead concentration. To disorder the material, the crystals were annealed at 1650 K for 20 min in sealed platinum tubes. Subsequent x-ray powder diffraction measurements revealed a degree of order of 0.5 from the (111) and (311) superlattice line intensities. After longer annealing times the crystals were found to show significant PbO deficit. They became opaque and were therefore not used for the scattering experiments. However, this limits our possibility of investigating more the disordered samples.

The Raman spectrometer consists of a 750 mW krypton laser light source with $\lambda = 647.1$ nm and a 30 mW He–Ne laser with $\lambda = 632.8$ nm. The beam was double-focused on the sample. In 90° geometry the scattered light was focused on the entrance slit of a Jarrel–Ash double monochromator and was detected with a Peltier cooled photomultiplier coupled to a photon counter. Simultaneously the signal was stored on an attached microcomputer for further line calculations. No evident influence of the polarisation direction of the laser beam was found while recording the spectra (presumably because of the depolarisation by the high number of domains). Therefore, only unpolarised spectra were recorded at different temperatures in the interval 102–873 K. Temperature regulation was reproducible to within 1 K above room temperature and 0.6 K at low temperatures. For two temperatures (102 K and 333 K) Raman spectra were first recorded over the spectral range from 5 cm^{-1} to 950 cm^{-1}. In a second experiment the profile of the most intense band in the low-frequency region of the spectrum near 61 cm^{-1} was measured as a function of temperature. For recording these spectra a 30 mW He–Ne laser was chosen to avoid local heating during the experiments.

The vibrational part of the profile follows from a quasi-harmonic response function (Bruce *et al* 1980) with the spectral density

$$g_{\mathrm{hm}}(\Gamma, \omega_\infty, \Omega) = i_0(n(\Omega) + 1)\Omega\Gamma/[(\omega_\infty^2 - \Omega^2)^2 + \Omega^2\Gamma^2] \tag{1}$$

where i_0 is a constant, Ω is the harmonic frequency, Γ the damping constant and $n(\Omega)$ the Bose–Einstein factor. Usually Γ represents an overall damping constant when multiphonon processes are taken into account. Following Salje (1986), disorder effects can give rise to further line broadening (density of states fluctuation) as phonons with wavevectors $q \neq 0$ are allowed to contribute to the spectral function.

The observed Raman profile is distorted due to the instrumental slit function s_{slit} according to the convoluted spectral function

$$g_{\mathrm{obs}}(\Omega) = \int_0^\infty g_{\mathrm{hm}}(\Gamma, \omega_\infty, \Omega)s_{\mathrm{slit}}(\Omega - \Omega')\,d\Omega. \tag{2}$$

The Raleigh line was used as the instrumental standard function. The fitting procedure was the same as that mentioned in the work of Bismayer (1988).

3. Phonon spectra of $Pb(Sc_{0.5}Ta_{0.5})O_3$ and their symmetry

The highest possible symmetry with the smallest unit cell in perovskite-like structures is $m\bar{3}m(O_h)$. As in the other perovskites like $BaTiO_3$, high-temperature disordered PST is of space group $Pm\bar{3}m(O_h^1)$ with $Z = 1$ (Groves 1985). However, for the high-temperature ordered PST, Randal *et al* (1986), from their electron microscopic studies, found a superlattice doubling of the unit cell which yields a face-centring of the lattice. Hence, the space group of the ordered paraelastic phase of PST is $Fm\bar{3}m(O_h^5)$ with $Z = 2$ for the equivalent primitive setting. Groves pointed out that the para-to-ferroelectric phase transition primarily involves non-equivalent shifts of the lead cations from their high-symmetry positions in the cubic phase along [111]. Salje and Bismayer (1989) have given the group-theoretical path (figure 1) of the phase transitions for both cases (disordered para to disordered ferro, ordered para to ordered ferro) as well as the Sc, Ta-ordering. Table 1 gives the correlation between different representations of the symmetry groups involved in the phase transitions.

Given below are the distributions of the $3n$ vibrational modes into various representations of the symmetry groups corresponding to high- and low-temperature phases.

(i) ordered para to ordered ferroelectric phase.

Paraphase $Fm\bar{3}m(O_h^5)$, $Z = 2$

$\Gamma_{tot} = A_{1g} + E_g + T_{1g} + 2T_{2g} + 5T_{1u} + T_{2u}$

$\Gamma_{acoust} = T_{1u}$

Ferrophase $R3m(C_{3v}^5)$, $Z = 2$

$\Gamma_{tot} = 8A_1 + 2A_2 + 10E$

$\Gamma_{acoust} = A_1 + E$.

(ii) disordered (Sc, Ta disorder) para to ferroelectric phase.

Paraphase $Pm\bar{3}m(O_h^1)$, $Z = 1$

$\Gamma_{tot} = 4T_{1u} + T_{2u}$

$\Gamma_{acoust} = T_{1u}$

Ferrophase $R3m(C_{3v}^5)$, $Z = 1$

$\Gamma_{tot} = 4A_1 + A_2 + 5E$

$\Gamma_{acoust} = A_1 + E$.

In case (i), the Raman active modes for the para phase are $A_{1g} + E_g + 2T_{2g}$, the Raman active modes for the ferro phase are $7A_1 + 9E$. In case (ii), according to group theory there are no Raman active modes in the para phase. The ferro phase Raman active modes are $3A_1 + 4E$.

Table 1. The correlation of Pb(Sc$_{0.5}$Ta$_{0.5}$)O$_3$ with space group F$\overline{m}$3m (para phase, $Z = 2$) and R3m (ferro phase, $Z = 2$) (top); space group Pm3m (para phase, $Z = 1$) and R3m (ferro phase, $Z = 1$) (bottom). IR = infrared active, R = Raman active, I = inactive.

F$\overline{m}$3m(O^5_h) $Z = 2$	R$\overline{3}$m(D$^5_{3d}$)	R3m(C$^5_{3v}$)
A$_{1g}$ (R)	A$_{1g}$	A$_1$ (IR, R)
E$_g$ (R)	E$_g$	E (IR, R)
T$_{1g}$ (I)	A$_{2g}$	A$_2$ (I)
	E$_g$	E (IR, R)
T$_{2g}$ (R)	A$_{1g}$	A$_1$ (IR, R)
	E$_g$	E (IR, R)
T$_{1u}$ (IR)	A$_{2u}$	A$_1$ (IR, R)
	E$_u$	E (IR, R)
T$_{2u}$ (I)	A$_{1u}$	A$_2$ (I)
	E$_u$	E (IR, R)

Pm$\overline{3}$m (O^1_h) $Z = 1$	R$\overline{3}$m(D$^5_{3d}$)	R3m(C5$_{3v}$)
T$_{1u}$ (IR)	A$_{2u}$	A$_1$ (IR, R)
	E$_u$	E (IR, R)
T$_{2u}$ (I)	A$_{1u}$	A$_2$ (I)
	E$_u$	E (IR, R)

4. Results and discussion

4.1. Ordered para to ordered ferroelectric phase transition

The Raman spectra of fully ordered PST in its ferroelectric phase at 102 K and that of the paraelectric phase at 333 K are shown in figure 2. Because of strong depolarisation effects due to micro-domains we did not separate the symmetry species of the unit cell vibrations. In agreement with the results of our factor group analysis we observe four prominent bands near 61 cm^{-1}, 240 cm^{-1}, 370 cm^{-1} and 830 cm^{-1} in the high-temperature phase of ordered PST. We see additional weak bands near 150 cm^{-1} and 540 cm^{-1} in the same phase. In the low-temperature phase there appear new symmetry allowed bands after the phase transition ($T_c \simeq 305$ K). The additional weak features in the paraphase spectrum can be attributed to residual local distortions of the rhombohedral symmetry. The striking feature in figure 2 is the line splitting in the region of the low-energy phonon branches. Consequently investigation was focused on the temperature evolution of the strongest band at 61 cm^{-1} of the low-temperature phase. In figure 3 the temperature dependence of the strong low-frequency band along with its neighbours is displayed. Figure 4 shows the variation of the integrated intensity, full width at half maximum and the square of the frequency as a function of temperature for the 61 cm^{-1} band.

The squared frequency of this phonon branch decreases linearly with increasing temperature from 102 K to 305 K. The integrated intensity of the chosen band increases linearly as it is heated from 102 K to T_C ($\simeq 305$ K); above T_C the intensity remains almost constant. The temperature dependence of the line width (Γ) far below T_C can be attributed to cubic and quartic anharmonic effects. This can be approximated by

$$\Gamma_{anh} = a + bT + cT^2. \tag{3}$$

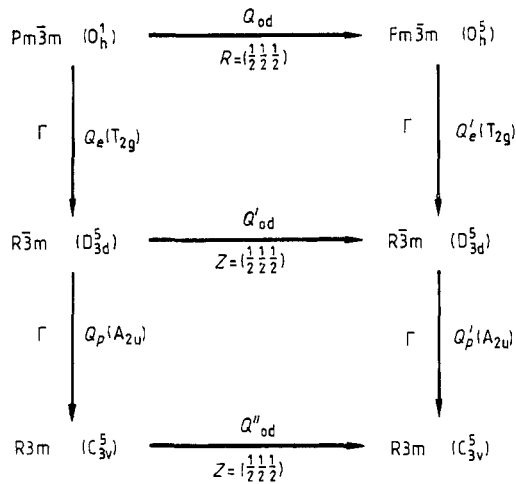However, just below and above T_C, the observed linewidth displays deviation from the

Figure 1. Correlation between the space groups involved in structural phase transitions in the relaxor material $Pb(Sc_{0.5}Ta_{0.5})O_3$. The arrows indicate the direction in which the symmetry is reduced. At each arrow the relevant order parameter Q and the critical point in the Brillouin zone of the respective high-symmetry form is given. Q_{od} represents the ordering of Sc and Ta atoms at the B sites; Q_e is the ferroelastic and Q_P the ferroelectric order parameter. The active representations are shown in brackets next to the order parameters (after Salje and Bismayer 1989).

anharmonic background. The lattice distortion leads to a significant linear decrease of the frequency ω^2 with increasing temperature from 102 K to $T_C \simeq 305$ K. $\Delta\omega$ is about 5 cm^{-1}. Consequently, the mode Grüneisen parameter (Munn 1975, Bismayer *et al* 1986) is expected to be somewhat large. The accompanying lattice distortion may be attributed to the ferroelastic deformation expected to be present in this system (Salje and Bismayer 1989).
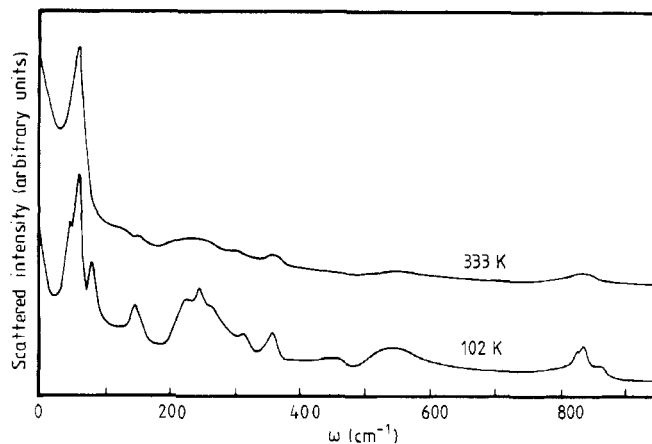

Figure 2. Unpolarised Raman spectra of fully ordered PST at 102 K (ferro phase) and 333 K (para phase).
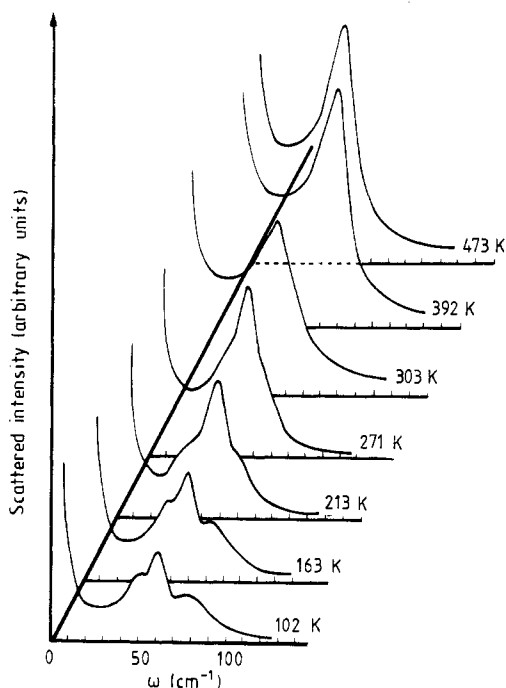
Figure 3. Unpolarised low-frequency Raman spectrum of fully ordered PST at different temperatures; the transition temperature is at about 305 K.

The linear increase of the integrated intensity as a function of temperature below T_C suggests that the intensity varies as the square of the order parameter. If the observed band is attributed to A_1 species which is both Raman and IR active in the low-temperature phase, such a behaviour is natural (Bismayer 1988, Groves 1985).

The maximum deviation of the observed linewidth from the anharmonic background is about 2 cm^{-1} above T_C. This suggests the presence of additional dynamic processes during the phase transition, in the high-temperature phase. These can be associated with the dynamical creation and annihilation of precursor (rhombohedral) clusters, cluster wall movements etc. (Bruce *et al* 1980, Salje *et al* 1983, Cross 1987). It is also interesting to notice that the extrapolated linewidth value at 0 K (figure 3) is about 6 cm^{-1} instead of being negligible. This can be explained by the fact that although the crystal is supposed to be completely ordered (Sc, Ta ordering) it is quite possible that minor disorder is present as it depends on annealing conditions. This disorder will lead to the density of states effect resulting in a finite linewidth.

4.2. Disordered para to disorderd ferroelectric phase transition

In figure 5 the temperature dependence of the strongest band at 61 cm^{-1} along with the neighbouring band is displayed. Figure 6 shows the plot of integrated intensity, full width at half maximum and the square of the frequency as a function of temperature for the 61 cm^{-1} band.

According to the selection rules of O_h^1 symmetry (high-temperature phase) no mode should be Raman active. Of course this is true only in a macroscopic sense. However,
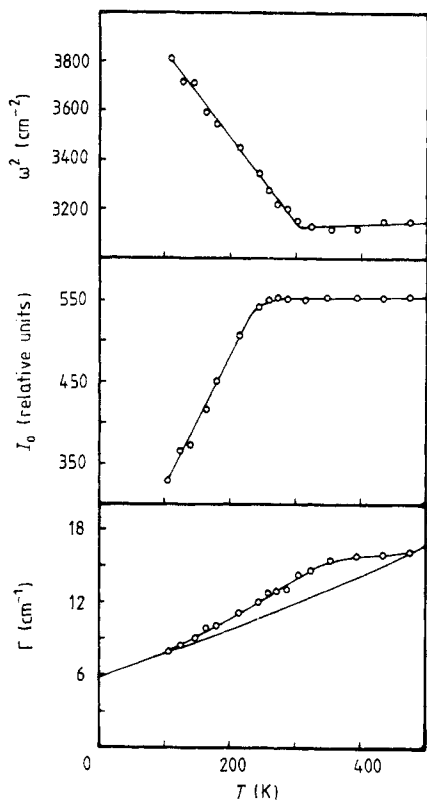
Figure 4. Frequency (ω^2) integrated intensity (I_0) and spectral linewidth (Γ) of the 61 cm^{-1} mode for fully ordered PST versus temperature.
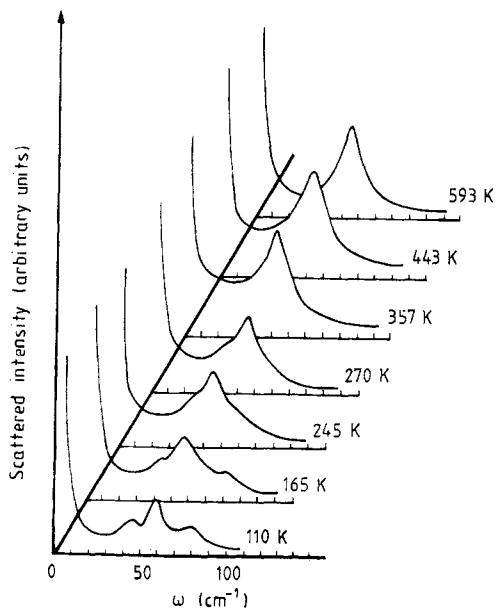

Figure 5. Unpolarised low-frequency Raman spectrum of disordered PST (the degree of order is 0.5) at different temperatures; the transition temperature is about 290 K.

because of the Sc, Ta disorder there will exist microscopic regions rich in Sc or Ta, thermodynamically in non-equilibrium, thus breaking the translational symmetry. This will give rise to Raman activity. Naturally the intensity of the Raman lines in the disordered para-phase crystals will be weaker than the Raman lines in the ordered para-phase crystals (see figures 3 and 5).

The integrated intensity of the 61 cm^{-1} band increases linearly as the temperature is increased from 102 K to T_C which is around 290 K (figure 6). The observed linewidth Γ shows a larger deviation from the anharmonic background below and above T_C when compared with the behaviour in the ordered crystal. The square of the frequency decreases with increasing temperature below T_C. Again the somewhat large associated Grüneisen parameter indicates larger lattice distortion which is to be correlated with the ferroelastic deformation due to the symmetry R$\overline{3}$m. The linear increase of integrated intensity with increasing temperature below T_C once again implies that the intensity varies as the square of the order parameter.

The larger maximum deviation of the observed linewidth from the anharmonic background (about 4.2 cm^{-1}, figure 6) shows that the presence of static compositional fluctuations (Sc, Ta) on a local length scale have a different impact on the dynamic precursors of the low-temperature rhombohedral phase. The extrapolated line width at 0 K is about 7.8 cm^{-1} which is higher than the value in the ordered crystal. This is to be expected because of the density of states effect due to the higher degree of disorder.

It is instructive to compare the temperature variation of linewidths in ordered and disordered crystals. Whereas the ordered crystal reveals a sharp phase transition the
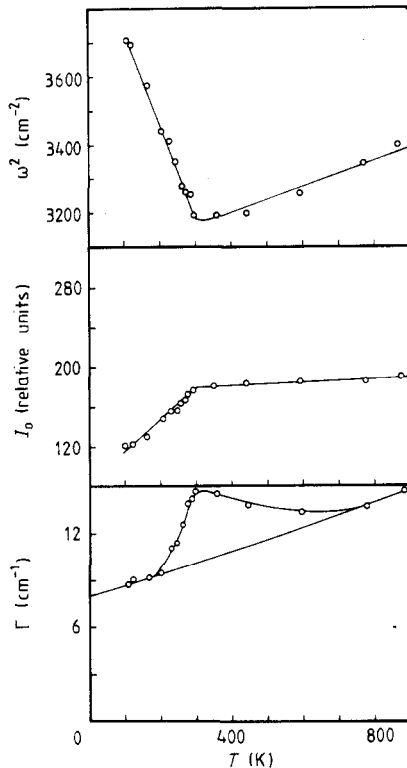

Figure 6. Frequency, integrated intensity and spectral linewidth of the 61 cm^{-1} band for disordered PST versus temperature.

disordered crystal is a relaxor ferroelectric with diffuse phase transition; i.e. the transition temperature is smeared out (Cross 1987). According to Groves (1985), it is primarily the displacement of lead atoms, which gives rise to the spontaneous polarisation, that leads to the phase transition. However, the lead atoms may displace in any one of eight directions. In the case of the disordered crystals this would mean polarisation domains being present above the mean T_C oriented in different directions. A comparison of figures 4 and 6 clearly reveals that whereas the deviation of the linewidth from the anharmonic background extends from about 120 K to 469 K for the ordered crystal, it extends from about 160 K to 750 K in the disordered crystal. This behaviour in the disordered material is in accord with the idea of Burns and Dacol (1983, 1986) who suggested that relaxor ferroelectrics make a transition to a glassy polarisation state from the para phase at a temperature that is much higher than the average ferroelectric transition temperature T_C.

Acknowledgments

References

Bismayer U 1988 *Physical Properties and Thermodynamic Behaviour of Minerals* (Nato ASI Series C vol 225) (Dordrecht: Reidel) p 143
Bismayer U, Salje E, Jansen M and Dreher S 1986 *J. Phys. C: Solid State Phys.* **19** 4537
Bruce A D, Taylor W and Murray A F 1980 *J. Phys. C: Solid State Phys.* **13** 483
Burns G 1976 *Phys. Rev.* B **13** 215
Burns G and Dacol F H 1983 *Solid State Commun.* **10** 853
—— 1986 *Solid State Commun.* **9** 567
Cross L E 1987 *Ferroelectrics* **76** 241
Devarajan V and Salje E 1986 *Phys. Chem. Miner.* **13** 25
Groves P 1985 *J. Phys. C: Solid State Phys.* **18** L1073
—— 1986 *J. Phys. C: Solid State Phys.* **19** 111
Munn R W 1975 *Phys. Rev.* B **12** 3491
Randall C A, Barber D J, Whatmore R W and Groves P 1986 *J. Mater. Sci.* **21** 4456
Reinecke T L and Ngai K L 1976 *Solid State Commun.* **18** 1543
Salje E 1986 *Phys. Chem. Miner.* **13** 340
Salje E and Bismayer U 1989 *J. Phys.: Condens. Matter* **1** 6967–76
Salje E, Devarajan V, Bismayer U and Guimaraes D M C 1983 *J. Phys. C: Solid State Phys.* **16** 5233
Setter N and Cross L E 1980 *J. Mater. Sci.* **15** 2478
—— 1981 *Ferroelectrics* **37** 551
Smolensky G A 1970 *J. Phys. Soc. Japan Suppl.* **28** 26
Smolensky G A, Siny I G, Pisarev R V and Kuzminov E G 1976 *Ferroelectrics* **12** 135
Stenger C G F and Burggraaf A J 1980 *Phys. Status Solidi* a **61** 275